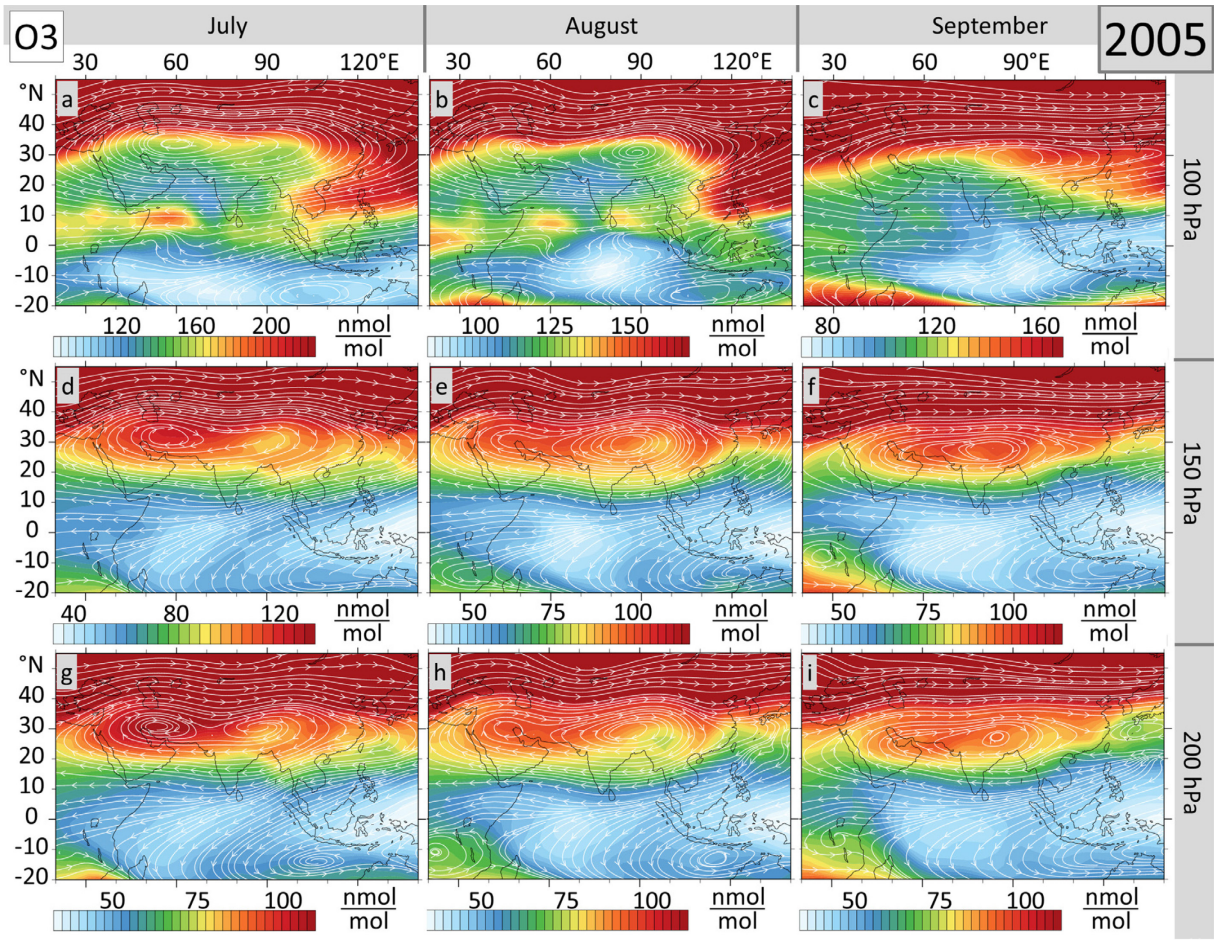

Figure S1: Monthly mean O_3 mixing ratios and streamlines in the ASMA region as simulated by EMAC for different pressure altitudes. The year 2005 was chosen for comparability with Park et al. (2007), who reported an O_3 minimum in the ASMA at 100 hPa for July – August 2005 (based on MLS satellite data). That feature is reproduced by EMAC, but O_3 is increased in the ASMA at lower altitudes.

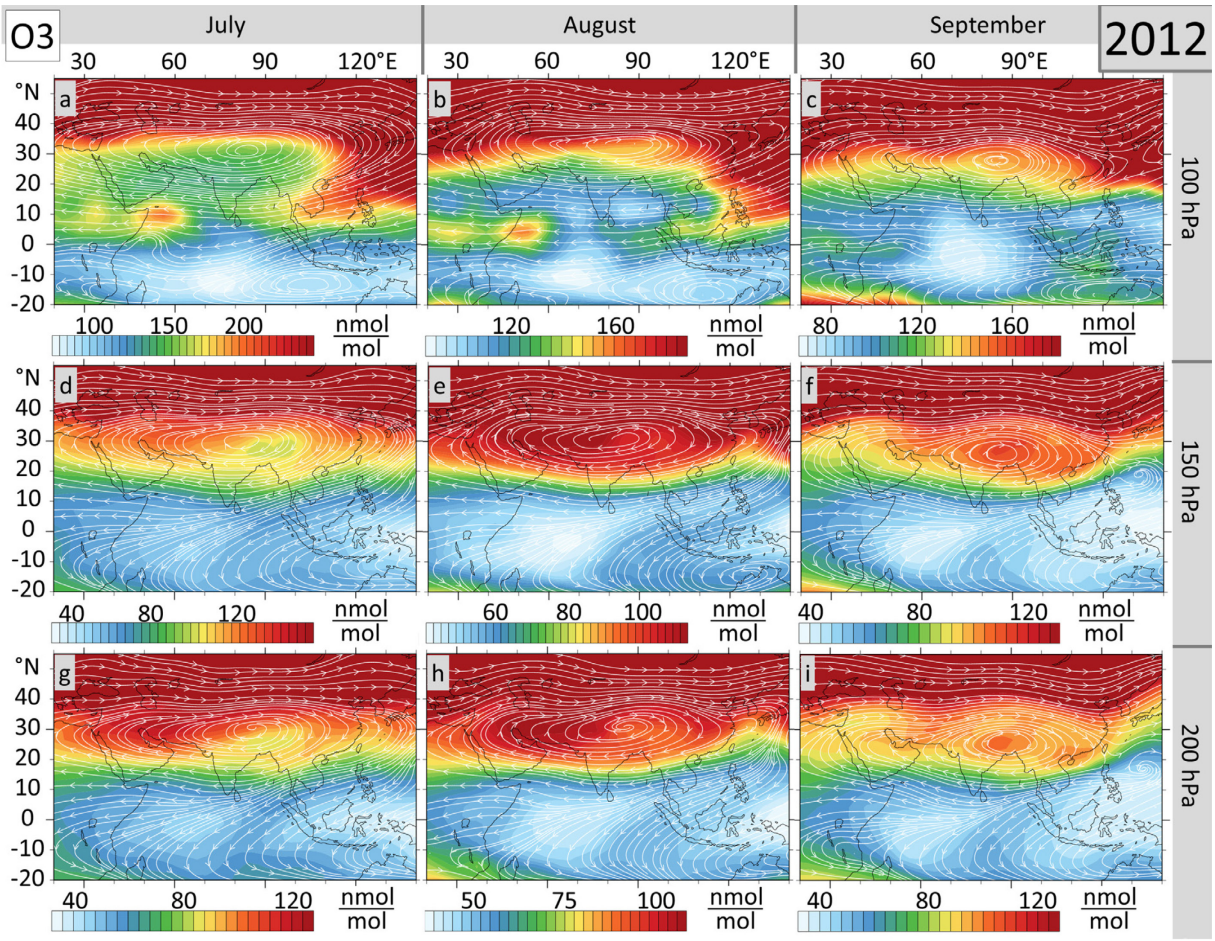

Figure S2: As Fig. S1, but for the year 2012. The main features are almost identical to 2005 (Fig. S1). O_3 is locally decreased in the ASMA only in July and August at 100 hPa. There are enhanced O_3 mixing ratios at lower altitudes throughout the monsoon season.

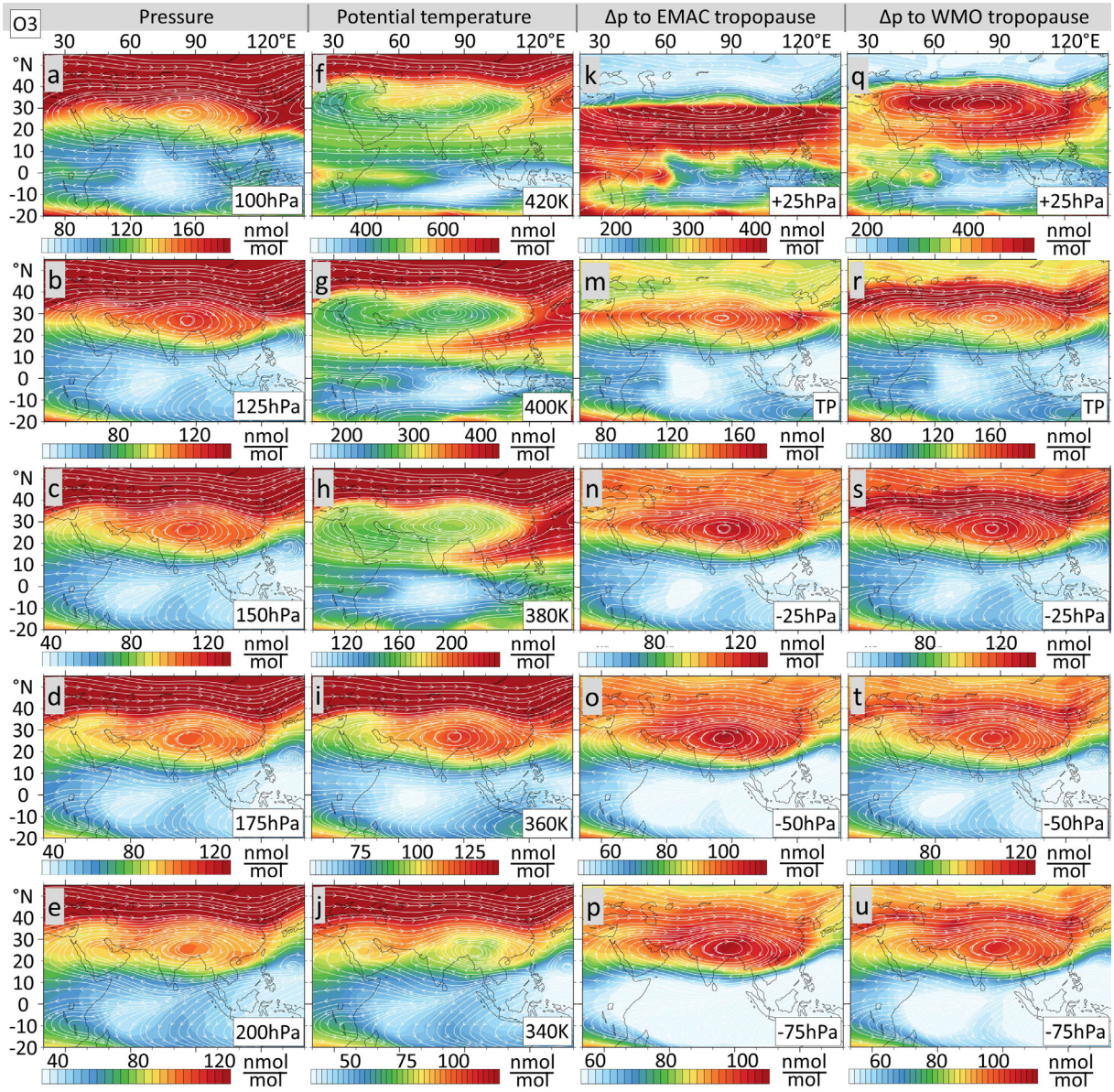

Figure S3: Monthly mean streamlines and O_3 mixing ratios in the ASMA region as simulated by EMAC for September 2012. Various levels are shown in different vertical coordinates to highlight two peculiarities. (i) Some studies report decreased O_3 in the ASMA interior on isentropic surfaces (Randel and Park, 2006; Kunze et al., 2010), while other analyses are on pressure levels (Park et al., 2007). Due to diabatic heating over the Tibetan Plateau, isentropes are concave there. They essentially form a trough when viewed in pressure coordinates (Ren et al., 2014). Thus it is more likely to find lower tropospheric trace gas signatures in the ASMA interior on a potential temperature surface than on a pressure level. (ii) The TP in EMAC is defined according to the WMO definition between 30°S and 30°N, and at a potential vorticity surface of 3.5 PVU otherwise. This might lead to discontinuities when viewing the ASMA region in terms of pressure distance (Δp) to the TP.

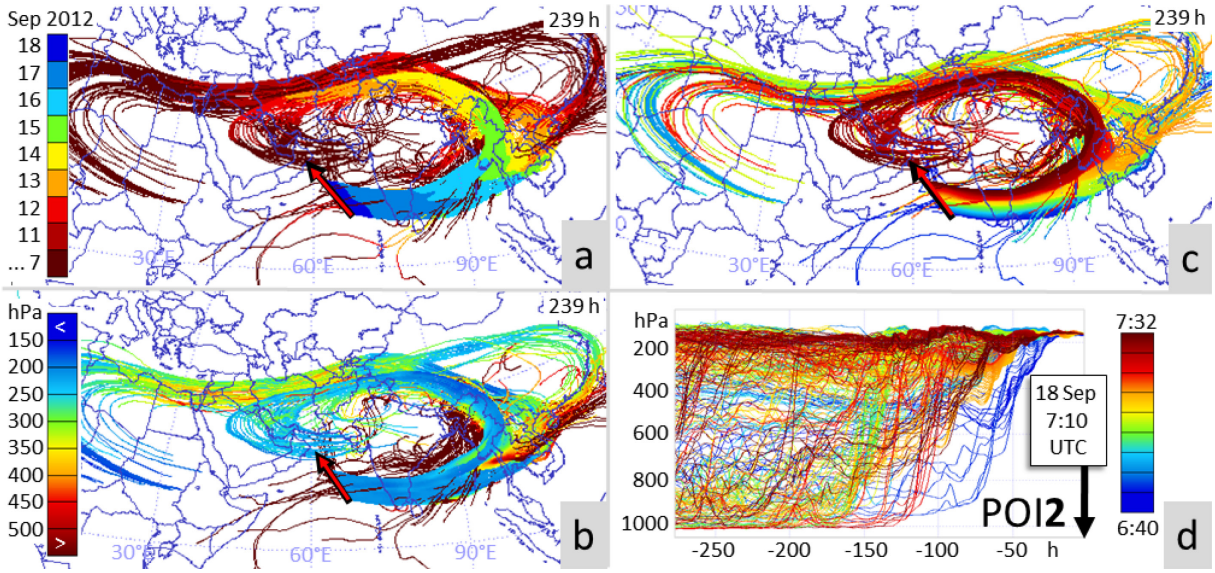

Figure S4: Backward trajectories starting at the HALO flight track (arrows). The integration length is noted in the upper right corner of each lat-lon panel. All trajectories of one panel start at the same time, approximately in the middle of the period corresponding to the respective flight segments (panels d, h, m). Colors in panels a, e, i relate the previous positions of the measured air parcels to calendar days. Colors in b, f, j show pressure altitude, which is supplemented by altitude vs time in d, h, m. Individual trajectories are color coded according to the time of measurement at their respective starting positions in all right columns' panels. POI2 covers the time after takeoff and ascend until encountering increased O_3 mixing ratios.

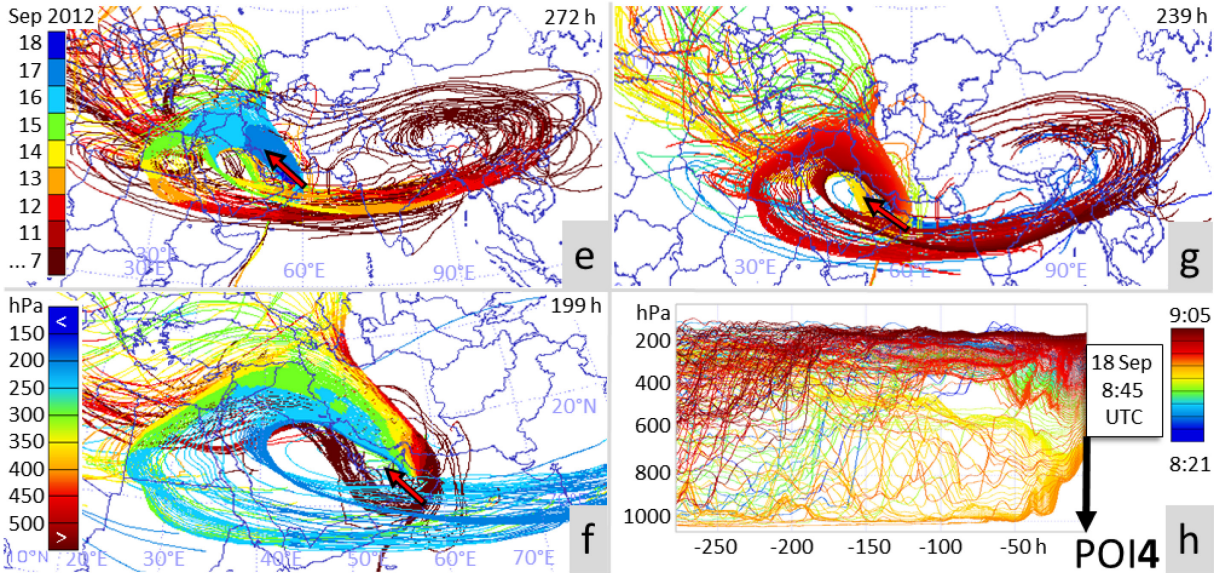

Figure S4: Continued for POI4, which is a dive from the UT into the middle troposphere. The interval for POI4 is chosen such that anticyclonic motion is much slower than in the above ASMA: Air from the highest altitudes of POI4 does not nearly circle the ASMA within 300 h, while air from POI3/5 needs about 200 h and 280 h, respectively (Fig. 3). The source regions contributing to POI4 primarily depend on the actual flight altitude, i.e. the sequence of air masses encountered during descend is mirrored during the following ascend.

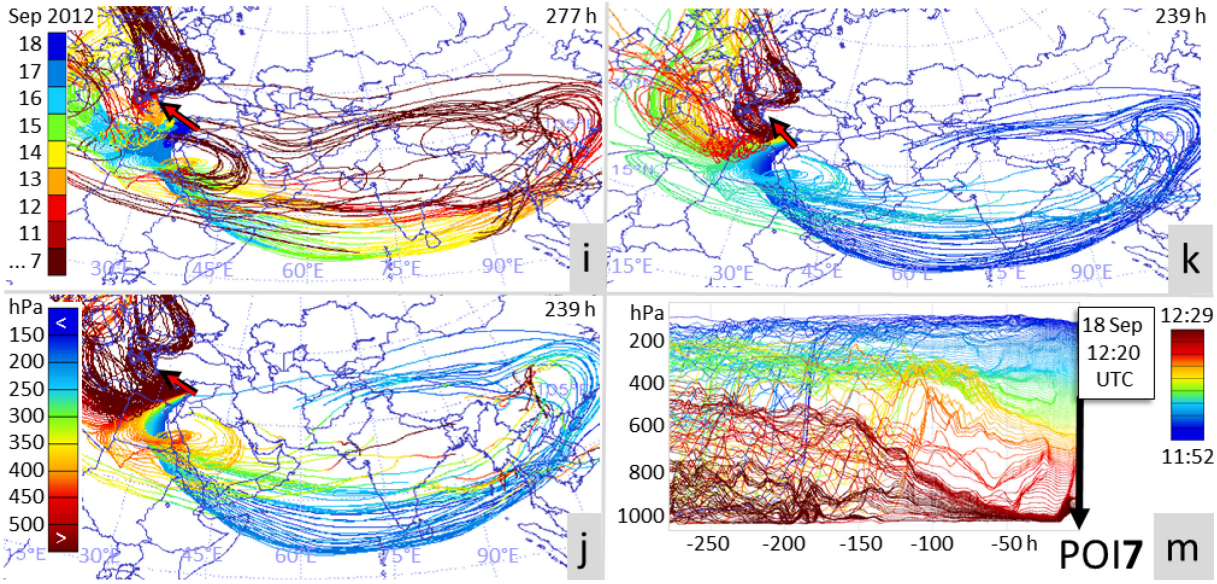

Figure S4: Continued for POI7, which covers the descend to Larnaca.

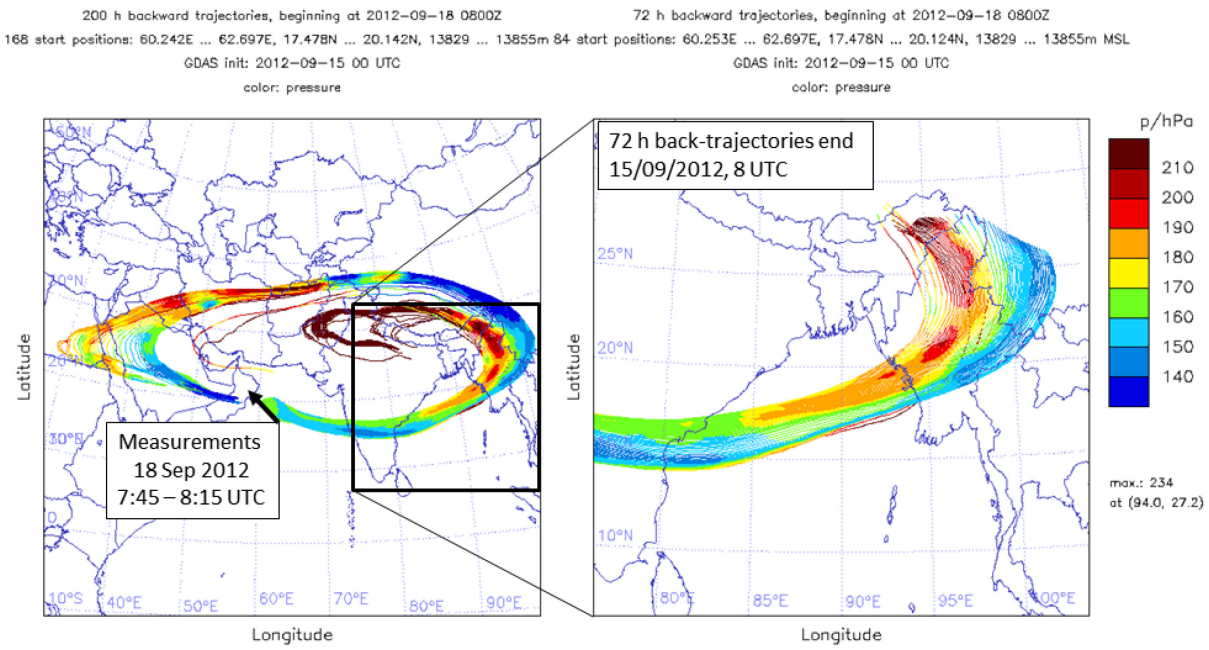

Figure S5: 200 hour (left panel) and 72 hour (right panel) backward trajectories with initial positions corresponding to 10 s steps along the HALO flight track. Colors indicate the pressure altitude of air parcels. UT anticyclonic circulation was entrained by a lower tropospheric upwelling at the eastern ASMA flank at about 15 September 2012, 8 UTC. Going back 72 hours, the transect measured by HALO corresponds approximately to an inclined zonal transect at 27°N.

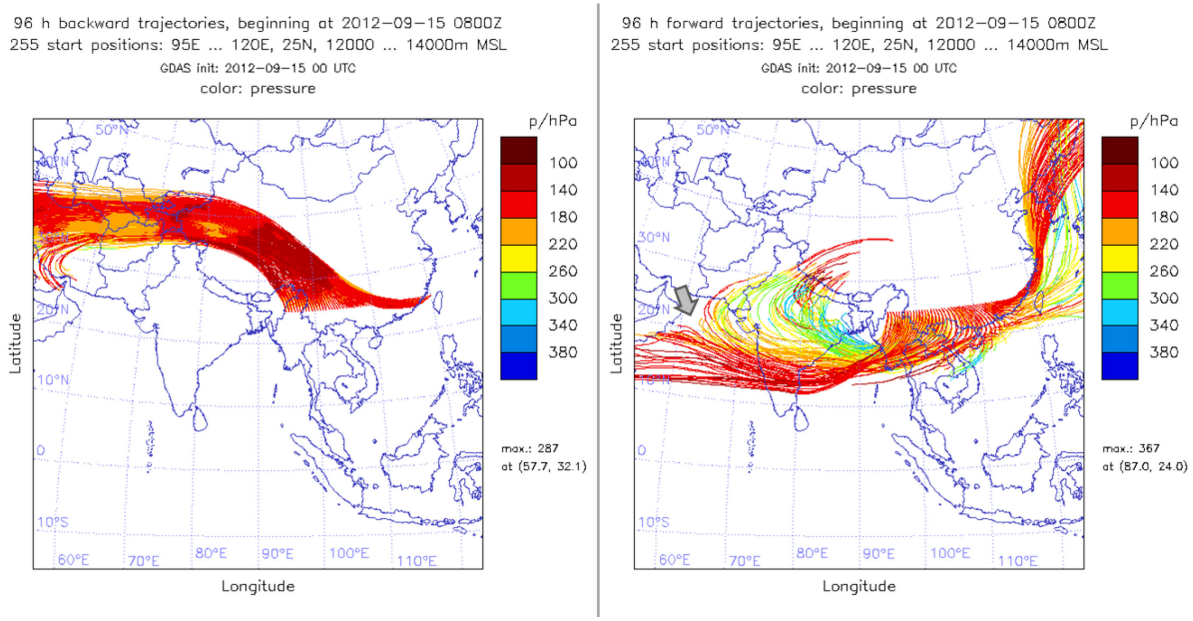

Figure S6: Four day backward (left) and four day forward (right) trajectories. The trajectories start from a plane intersecting the eastern ASMA edge when the air mass measured by HALO was there. The wind field is strongly divergent at the eastern ASMA flank. During the time covered by the trajectories the anticyclone split (right panel). A grey arrow marks where the flow is separated between the Tibetan and the secondary Iranian anticyclone.

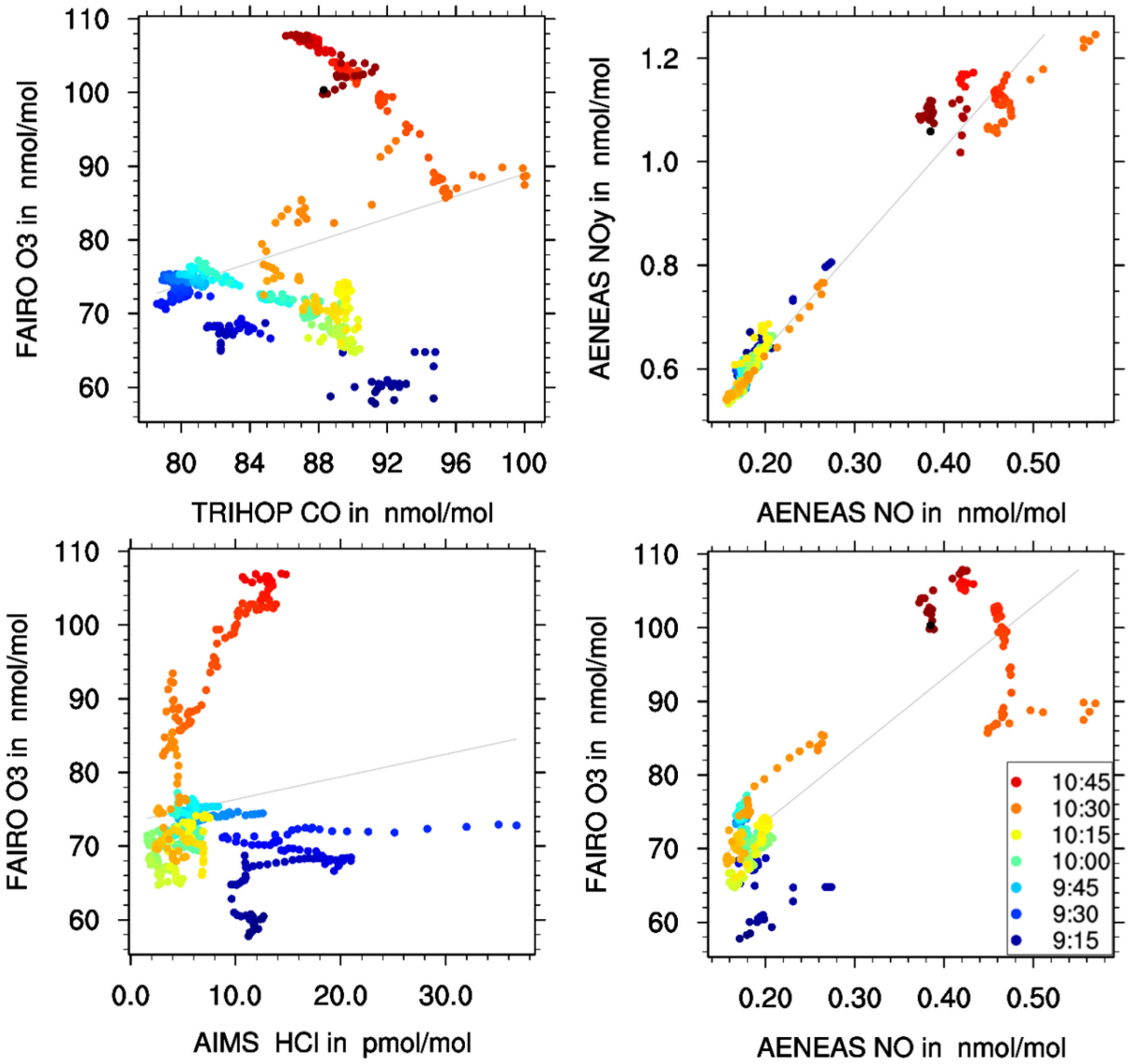

Figure S7: Tracer-tracer relations in the ASMA, as observed during POI5. Colors indicate the time of measurement, grey lines are linear fits to the data. These panels are shown here for completeness, to document the in-situ data for all POIs. They may be explained by the same processes discussed for POI3 in the main text, but are better viewed in the more climatological context of (Gottschaldt et al., 2016).

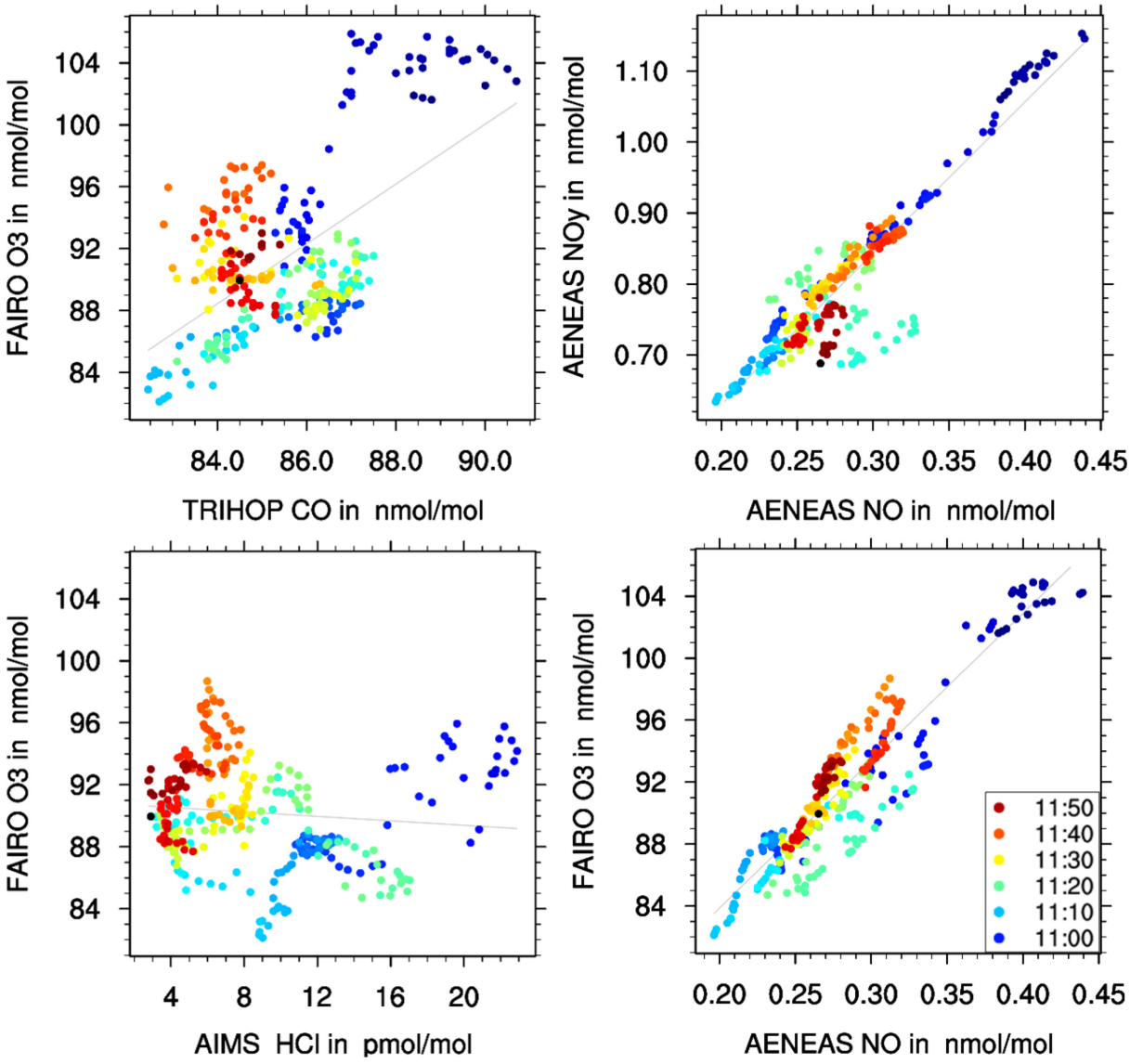

Figure S8: As Fig. S7, but for POI6.

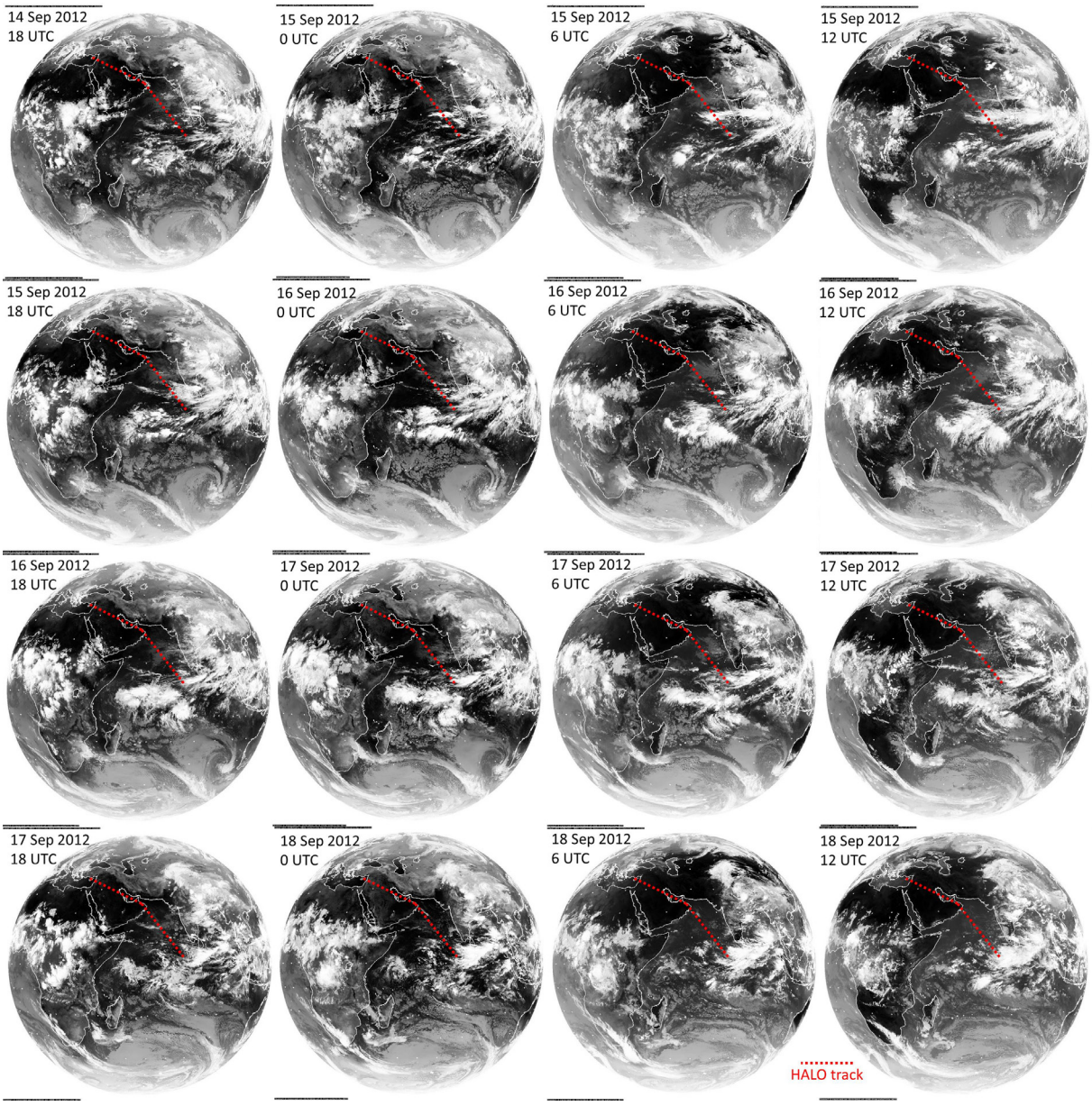

Figure S9: Meteosat-7 (positioned 57°E, Indian Ocean Data Coverage) quicklook images for a 4-day period (14 – 18 September 2012) before the HALO ESMVal measurements in the ASMA (18 September 2012). The thermal infra-red channel (10.5 – 12.5 µm) is shown. Dark shadings correspond to cloud-free conditions, which prevailed at the HALO flight track during the entire period. Light shadings east of India indicate convection, which is consistent with upwellings at the eastern flank of the ASMA that were also seen in the corresponding back-trajectories (Fig. 3). All images are courtesy of the NERC Satellite Receiving Station, Dundee University, Scotland (www.sat.dundee.ac.uk).

References

Gottschaldt, K., Schlager, H., Baumann, R., Cai, D. S., Eyring, V., Graf, P., Hoor, P., Jöckel, P., Jurkat, T., Voigt, C., Zahn, A., and Ziereis, H.: A case study of composition and transport in the Asian summer monsoon anticyclone, Part 2: Model simulations, Atmos. Chem. Phys. Discuss., in prep., 2016.

Kunze, M., Braesicke, P., Langematz, U., Stiller, G., Bekki, S., Brühl, C., Chipperfield, M., Dameris, M., Garcia, R., and Giorgetta, M.: Influences of the Indian Summer Monsoon on Water Vapor and Ozone Concentrations in the UTLS as Simulated by Chemistry–Climate Models, Journal of Climate, 23, 3525-3544, 10.1175/2010jcli3280.1, 2010.

Park, M., Randel, W. J., Gettelman, A., Massie, S. T., and Jiang, J. H.: Transport above the Asian summer monsoon anticyclone inferred from Aura Microwave Limb Sounder tracers, Journal of Geophysical Research, 112, 10.1029/2006jd008294, 2007.

Randel, W. J., and Park, M.: Deep convective influence on the Asian summer monsoon anticyclone and associated tracer variability observed with Atmospheric Infrared Sounder (AIRS), Journal of Geophysical Research, 111, 10.1029/2005jd006490, 2006.

Ren, R., Wu, G., Cai, M., Sun, S., Liu, X., and Li, W.: Progress in Research of Stratosphere-Troposphere Interactions: Application of Isentropic Potential Vorticity Dynamics and the Effects of the Tibetan Plateau, J. Meteor. Res., 28, 714-731, 10.1007 /s13351-014-4026-2, 2014.